A Vision System for the Online Quality Monitoring of Industrial Manufacturing

Giuseppe Di Leo, Consolatina Liguori, Antonio Pietrosanto, Paolo Sommella
Department of Industrial Engineering (DIIn) - University of Salerno
Via Giovanni Paolo II, 132- 84084 Fisciano (SA), Italy
e-mail: {gdileo, tliguori, apietrosanto, psommella}@unisa.it

***Abstract*— The design of an image based measurement system for the online inspection of electromechanical parts is described. A two-camera architecture is introduced in order to highlight all the required details involved in the measurements. The design takes into account both the interfacing and the real-time issues that assure an effective online operation. The description of the measurement system and the corresponding installation on the production line points out a methodological approach to the design of these kinds of measurement systems. The paper provides details about the algorithms for the localization and the measurement of the required quantities, as well as the calibration procedure and the error correction. Experimental tests for the performance evaluation are presented and discussed in terms of timing and accuracy.**

Keywords—metrology, visual inspection, online measurement, contact-less measurement, uncertainty;

I. INTRODUCTION

Industrial production is strongly interested in the advantages offered by image-based measurement systems for product inspection: contact-less inspection of products means reduction of invasiveness, reduction of costs, more favorable sampling of parts, statistical significance of the results and better awareness of the operators about the line operation conditions [1]-[5]. Traditional areas, where artificial vision systems have been successful, include the contactless inspection of manufactured goods such as automobiles, semiconductor chips, food and pharmaceuticals. The goal is to reduce the production costs due to human intervention in the defect analysis or due to the discard of defective parts by ensuring consistent product quality [6]. Image-based systems can also automate the manufacturing processes by controlling equipment such as industrial robotic arms. In many cases, the process parameters can be tuned through a feedback network, which modifies the parameters of the industrial process as soon as a trend is detected which would give raise to defects if it were not promptly compensated.

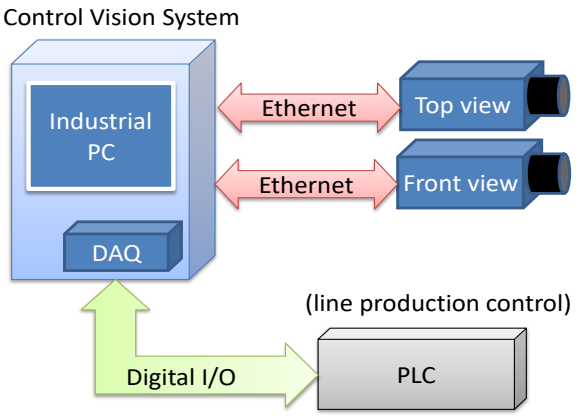

Figure 1: The measurement system

Machine vision systems have also taken an important role for the measurement of the mechanical (stamped metal) components to ensure that the corresponding parts fall within given specification limits. The key to their success can be found in distinctive attributes such as flexibility, reliability, higher operating speeds, consistency and accuracy, which have made them competitive if compared to traditional measurement systems.

The development of the artificial vision system is strongly influenced by design models based on the reuse of widely-adopted software library components and on general-purpose vision hardware. Consequently, the chosen application architecture and the algorithms adopted in the single processing stages are often depending on previous experience and trial iterations that eventually lead to the final tuning of the automatic system.

In order to optimize the development cycle, this paper intends to introduce a more schematic and progressive approach to the design of vision-based measurement system in the industrial context: the adoption of simple rule-based sequence of decision is proposed aiming to improve both the phases of the calibration and the evaluation of measurement uncertainty.

Following the approaches suggested by the scientific literature [7]-[10] about the image based measurement systems for industrial application, camera calibration as well as the analytical calculation and correction of systematic effects may be carried on according to a well known framework.

Under this point of view, the specific proposed measurement system will act as a case study for the demonstration of the approach. The measurements performed by the proposed automatic system in order to check the matching of the electro-mechanical parts to the manufacturing requirements can be grouped into different classes: i) widths and heights of given parts, ii) distances between lines to be located and

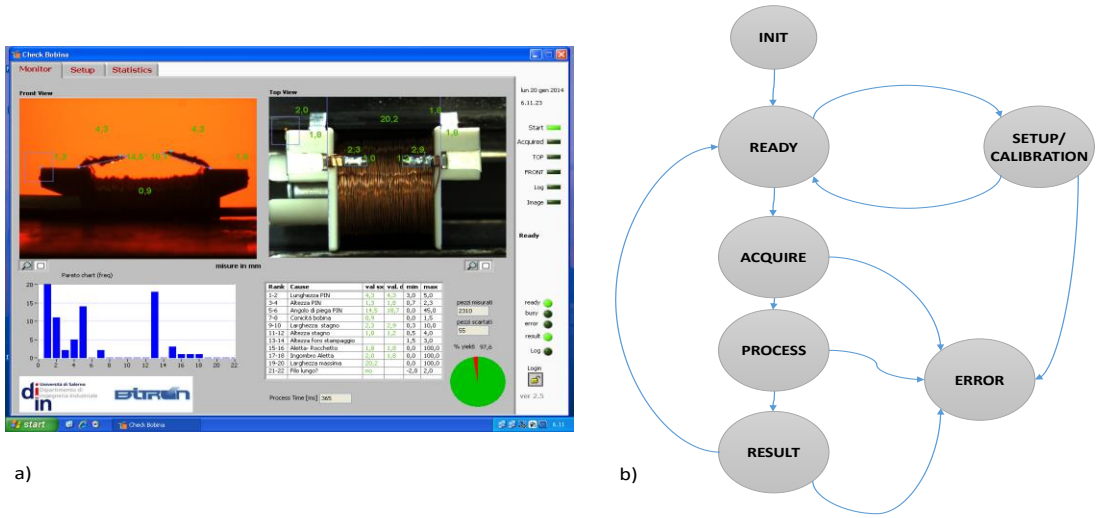

Figure 2(a) The main screenshot and the (b) state diagram of the application

reference lines; iii) angles between lines to be located and reference lines; iv) presence of unwanted defects.

In the following, after a description of the overall structure of the measurement station, the procedures for the calibration, for the measurements and for the error correction are presented in terms of an extensive experimental verification. For each one of these aspects, the criteria which eventually led to the design choices will be detailed.

II. System Description

The proposed measurement system allows the detection of defects and the dimensional monitoring of electromechanical parts, which include conducting wires and plates put onto plastic or metal supports and leverages, with different employments in appliances and devices, such as interrupters or locks. The traditional control of all the pieces produced is carried out by an operator. The pieces at the end of the production line are arranged into a matrix support containing 25x20 pieces; the typical defects are detected by the operator inspection through a magnifying lens. Periodically a single piece is checked by the laboratory quality.

The introduction of the proposed system has allowed to check online all the produced items. The measurements of each piece are compared to reference values and, whenever they are outside the given tolerances, the piece is discarded. The measurement system is positioned at the end of the production line at Bitron plant in Alatri, Italy. It is composed by two cameras connected via Ethernet bus to a control industrial PC. The system components are shown in Figure 1. Two cameras, hereinafter labeled *top* and *front*, are needed because the lengths to be measured can be observed on two different sides of the product. There is also a National Instruments data acquisition board NI PCI-6601 connected to the processing unit through the USB bus; its digital I/O lines are used for the information exchange with the PLC (Programmable Logic Controller) that manages the production line. For each piece the following sequence of tasks is operated by the system:

- waiting for a new piece (see section II.B);
- image acquisition from the top camera;
- turning on the backlight illuminator (see section II.A);
- image acquisition from the front camera;
- automatic image processing;
- visualization of the results.

The software was developed in LabVIEW; the main screenshot of the application is shown in Figure 2a); while the state diagram of the application is depicted in Figure 2b). In the following, specific aspects related to the metrological issues are detailed.

Two images are acquired by two Imaging Source DFK 23G445Gigabit Ethernet cameras, equipped with a Sony ICX445AQA progressive scan CCD sensor.

The interline CCD solid-state image sensor has a diagonal of 6.0mm (Type 1/3") with a square pixel array and 1.25M effective pixels. Progressive scan enables all pixel signals to be output within 1/22.5 seconds. The image size is 1280 x 960 pixels. Both cameras use a Fujinon lens CF25HA-1 with a focal length of 25 mm, an F/number of 1:1.4, an iris range of [1.4, 22] and a minimum object distance of 0.1 m.

The lighting system consists of an LED backlight illuminator, which can be programmatically switched on and off, and an

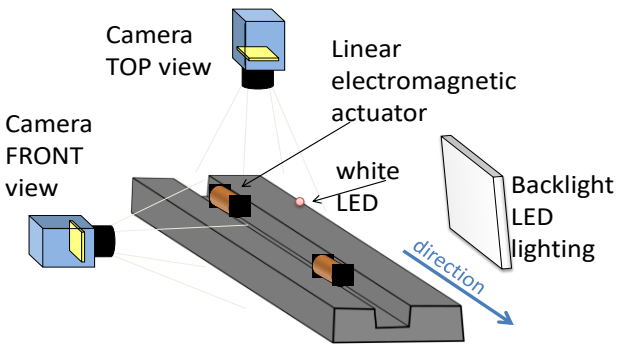

Figure 3: Position of cameras and illuminator with respect to the object under inspection

additional single white LED.
The layout of the components of the vision system is shown in Figure 3. As previously introduced, for each piece under measurement two images are acquired respectively by the top view and front view camera. The white LED is constantly lit to weakly illuminate the piece from a direction opposite to that of the front camera, while a backlight illuminator is activated only during the image acquisition by the front camera.

III. THE VISION PROCEDURES

The images acquired by top and front cameras undergo two completely separated processing procedures. They will be described in the following.

A. Top Image processing

The aim of this task is the measurement of the lengths L_1, L_2, L_3, L_4, and L'_2, L'_3, L'_4, which are deemed critical in the design specifications. Furthermore, the width L_5, L'_5 and height L_6, L'_6, of the tin-plated area of the metal blades are measured. All dimensional measurements are shown in Figure 4. The algorithm was developed using typical image processing functions. In particular, functions of the library NI Vision by National Instruments have been adopted. All the measurement functions are applied to associated rectangular regions of interest (ROIs) defined by the user relative to a main reference coordinate system anchored onto the left top corner of the object (shown as two arrows in red in Figure 4).
The main steps of the algorithm for top image processing are the following:

- extraction of luminance and saturation planes from RGB input image;
- application of morphological and thresholding operators to the luminance image to compensate minor variations in brightness;
- search for the location and orientation of the main reference coordinate system (whose purpose is *i)* to detect possible minor changes of the object position in the image with respect to the expected position and *ii)* to compensate them by accordingly roto-translating the ROIs;
- search for straight lines approximating edges to be used as reference lines (dotted green lines in Figure 4), r_1, …, r_7 , r'_1, …, r'_7, for the length measurements. The search for these lines is performed with a two step procedure: i) localization of the edge points along a set of search lines (horizontal o vertical) within the search region; ii) calculation of the orthogonal best fit line for the detected edge points.
- measure L_1, L_2, L_3, L_4 and L'_2, L'_3, L'_4 (shown in the Figure 4) as the distance between a proper pair of reference lines.
- measure L_5 and L_6 as the width and the height, respectively, concerning with the part of the tin-plated metal blade element. They are detected using a function that thresholds the image to isolate objects from the background and then locates, counts, and measures objects in a rectangular search area. This research is performed on the Saturation plane of the image (an example is shown in Figure 5). It was experimentally verified that the saturation component is the one that best highlights the difference between the copper and tin.

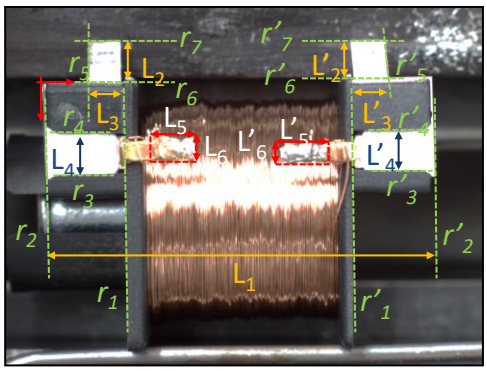

Figure 4: Measurements on top image

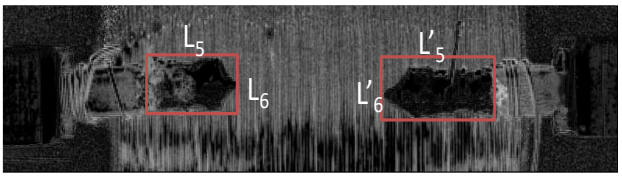

Figure 5: Detection of tin-plated metal blades

B. Front Image processing

The procedure allows to achieve measurements on those parts not visible from the top view. In more details, focus is devoted to the overall dimensions of the metal blades, the corresponding angles of inclination and the taper ratio of the coil, as shown in Figure 6.
The front image is acquired using a backlight illuminator. A binary image is created with a threshold. The threshold is equal to 75% of the value of the average brightness in a fixed area of the background. The main steps of the algorithm of the front image processing are the following:

- search for the location and orientation of the reference coordinate system for the front image (shown as two red arrows in Figure 6). The correct positioning of this

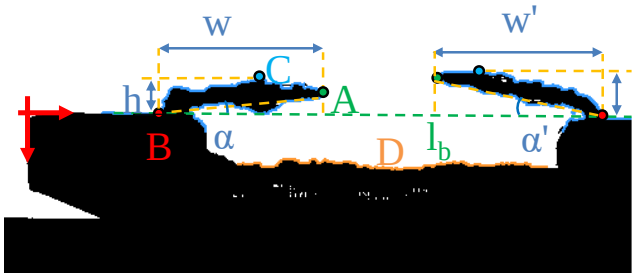

Figure 6: Reference coordinate system (red arrows) and measurements on front image

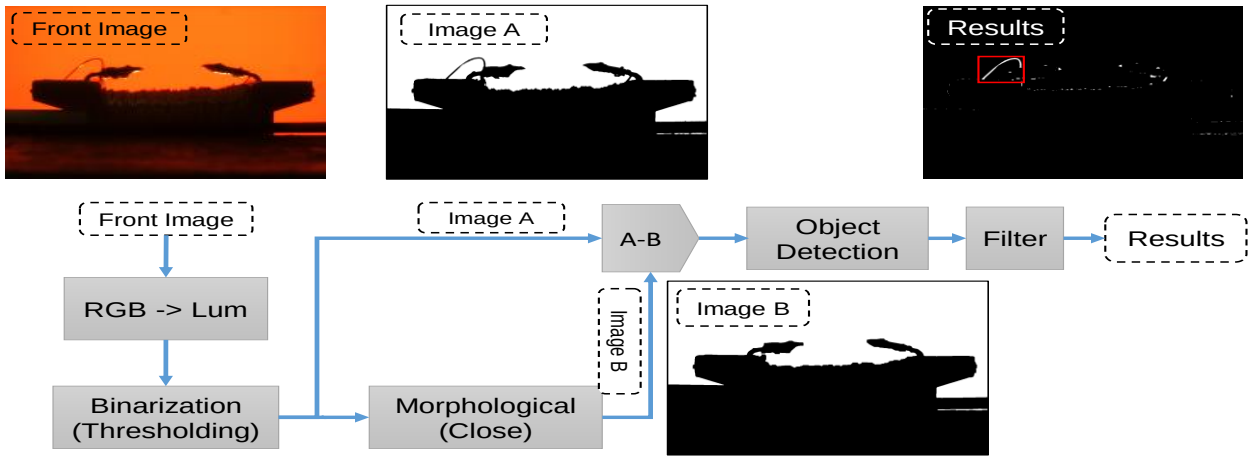

Figure 7: Diagram of the algorithm for detection of loose cooper wire

reference coordinate system is very important because in the front-image the ROIs are roto-translated in order to maintain a fixed relative position to the reference coordinate system. In this way, possible small displacement of the object with respect to the camera are taken into account and compensated;

- search for the baseline l_b (dotted green lines in Figure 6), determined as a least square line that best fits the almost-horizontal contour points on the left of the left blade and on the right of the right blade;
- extraction of the contour points (blue points in Figure 6) concerning with the left and right metal blade. Contour curve is a set of edge points that are connected to form a continuous contour;
- process of the contour points for the search for the singular points *A*, *B*, *C*. Point *A* and *C* are defined as the rightmost and the topmost point, respectively, of the blade contour. Considering the left blade, tracking the contour starting from left, *B* is defined as the first point with slope greater than zero. The slope is defined with respect to the baseline l_b. Because A and B are needed in order to measure the angles between straight parts, a careful choice and localization of these two points is important. After having observed the variability of the actual shape of the blade in many pieces, different solutions based on linear least squares were discarded because of the high variability of the blade thickness. The tip extrema A showed a much more stable behavior and was chosen;
- measurement of: the angle α between the baseline l_b and the segment *BA*; the length *w* estimated as the projection of the segment *BA* onto the baseline l_b; the length *h* estimated as the projection of the segment *CB* onto the normal to the baseline l_b. Similarly the quantities α', *w'* and *h'* are measured on right metal blade;
- measurement of the taper ratio *D* of the coil, namely the difference between the maximum and the minimum vertical coordinates of the contour points taken on the coil.

C. *Loose Wire Detection*

The target of this procedure is searching for a specific defect [11]: the presence of loose copper wire due to errors in the coil production. As schemed in Figure 7, the proposed algorithm includes the following steps:

- A pre-processing of the color input image to obtain a binary image (Image A) by: (i) color to monochrome image conversion, (ii) image binarization using an adaptive threshold.
- Creation of image B by applying to the image A a morphological closing operator with a structuring element of 15x15.
- Subtracting image B from the A.
- localization, counting and measurement of the objects in the image. This function uses a threshold on the pixel intensities to segment the objects from their background.
- Filtering and selection of objects found. The possible loose wire may only stay above the base line and must have a minimum size.

Some of these processing steps are very time consuming, such as morphological and convolution operations. In order to speed up the elaboration, whenever possible, masks have been introduced so to perform the processing only within them.

IV. METROLOGICAL ISSUES

A. *The calibration*

For both cameras, the relative geometry between camera and object is rigidly constrained. In more details, the working distance, defined as the distance between lens center and object, can be considered constant. For this reason, a simpler model for the camera has been adopted [12], [13]. The low number of parameters of the model to be determined and the low complexity of the calibration, allows to reduce the influence of uncertainty sources and to avoid the numerical instability of certain calibration algorithms. Basically, two scale coefficients, β_x and β_y, for the horizontal and for the

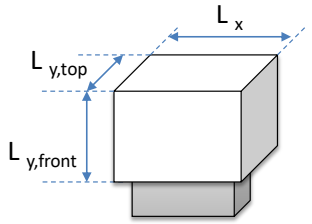

Figure 8: Calibration block

vertical direction, respectively, are introduced in order to relate the metric transversal coordinates of the real point and the pixel coordinates of its image:

$$\begin{cases} d_{mx} = \beta_x \cdot u \\ d_{my} = \beta_y \cdot v \end{cases} \quad (1)$$

The coefficients β_x and β_y, expressed in mm/pixels, have to be evaluated during a calibration phase, which requires the acquisition of a single image for each camera of a calibration block (Figure 8), whose characteristic dimensions L_x and L_y are known with a given accuracy. The vertical reference dimension L_y is different for the two views: it is either $L_{y,top}$ for the top view or $L_{y,front}$ for the front view. In the following, a general procedure will be described that can be applied separately for both views, provided the proper L_y is chosen. A processing routine based on least squares estimation extracts from the image the lengths in pixels, L_u and L_v, of these two same dimensions. Then eqs. (1) are solved for β_x and β_y:

$$\begin{cases} \beta_x = L_x / L_u \\ \beta_y = L_y / L_v \end{cases} \quad (2)$$

The calibration block is positioned in front of the cameras so that the distance z_{cal} between the lens and the surface of the reference object, where the dimensions are taken, is approximately equal to the average of the maximum and minimum distances associated to the measurements to be taken on real objects.

B. Systematic depth error correction

In this section analytical details are given about the measurements and the correction of the errors due to the non-planarity of the object.

After having evaluated the scale coefficients, the measurement of a length can be performed as a Euclidean distance between two points expressed as a (d_{mx}, d_{my}) pair, evaluated with eqs.(1). Since all the measurements are taken along either horizontal or vertical direction in the considered application, the horizontal and the vertical equations will be kept separated. When the length under measurement lies on a plane at a distance $(z_{cal} + \Delta z)$ from the camera different from the distance z_{cal} adopted during the calibration, an error occurs. The horizontal component of that error, e_x, is shown in the view depicted in Figure 9. The term γ_x is the horizontal component of the angle between camera axis z and the line of sight connecting the imaged point at camera horizontal coordinate x_P and its image at pixel horizontal coordinate u_P. The term f is the camera constant, approximately equal to the lens focal length.

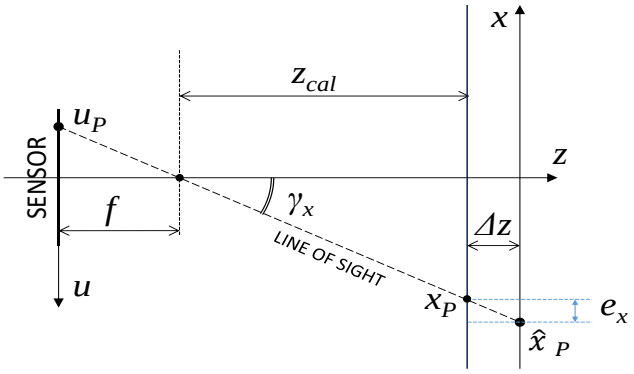

Figure 9: Error due to depth variation

Introducing the horizontal pixel density k_u as the inverse of horizontal cell size (typically between 3 µm and 7 µm for most industrial cameras) and expressing k_u in pixels/mm, the following relationship can be written:

$$e_x = \Delta z \cdot tg(\gamma_x) = \Delta z \frac{u}{k_u f} \quad (3a)$$

Substituting the values of the devices described in Section IIB, k_u = 1/(3.75 µm/pixel) = 266.6 pixels/mm, f = 25 mm, and estimating an absolute maximum deviation for Δz equal to 5 mm, for a point imaged at the maximum u = 1280/2, namely at the border of the image, the maximum error e_x is equal to 96 µm, then less than 0.1 mm. A similar relationship states for the error along the vertical direction e_y:

$$e_y = \Delta z \cdot tg(\gamma_y) = \Delta z \frac{v}{k_v f} \quad (3b)$$

The substitution of actual parameters gives: $|e_y| \leq 58$µm. Since (e_x, e_y) are systematic in nature, when the Δz at which the real point is expected to lie is known, as in the present case, then eq.(3a) and (3b) can be used in order to determine the corrected estimations of metric lengths, d_{cx} and d_{cy}, from the uncorrected ones, d_{mx} and d_{my}, estimated as in eqs.(1):

$$\begin{cases} d_{cx} = d_{mx} - e_x(\Delta z, u) \\ d_{cy} = d_{my} - e_y(\Delta z, v) \end{cases} \quad (4)$$

V. Metrological Verification

In order to evaluate the metrological performance of the proposed measurement system a black box approach was followed both for all types of measurements. To this aim, suitable validation sets of electromechanical pieces were collected and repeated observations were made on this set.

In the following the performances for all quantitative measurements and for the presence of a loose copper wire are detailed in two separate subsections.

A. Quantitative measurements

The measurements of interest are 18: 11 are made on the top image, including 7 length measurements (L_1, …, L_4, L_2', …,

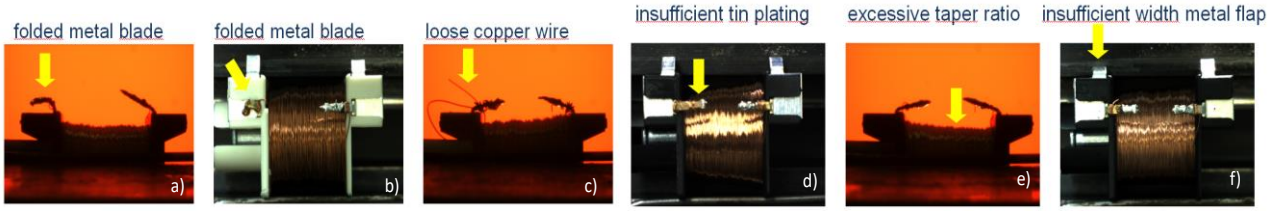

Figure 10: Examples of different kinds of defects

L_4') and 4 refer to the dimensional measurements (L_5, L_6, L_5', L_6') of the tin plated metal blades, whereas 6 the geometrical characteristics of the two metal blades (α, w, h and α', w', h') and the taper ratio D are measured on the front image. The validation set was suitable composed by 50 pieces, in order to reproduce a wide range of production behavior. In more details, the validation set was composed such that the 30% of the pieces satisfy all the specifications while the other pieces do not satisfy at least one specification.

In Figure 11, some example images of the validation set are shown. The reference measurements were manually obtained by an expert quality operator.

The validation pieces were sequentially put at the end of the production line and processed by the proposed system; this single sequence of measurement was repeated 30 times. For each piece, the obtained measurements were compared with the reference ones and the errors were calculated. In Table I the results were summarized in terms of:

- correct detection percentage (CD) evaluated as the ratio between the number pieces for which the averaged (on 30 repeated tests) measured value is compatible with the reference one, and the number of pieces;
- missed detection percentage (MD), i.e. the number of pieces out from the specification (in terms of reference value) for which the measured value matches the tolerance, with respect to the number of test set,
- false alarm rate (FD), evaluated as the number of pieces within the specification range (in terms of reference value) for which the measured value do not match the tolerance, versus the number of test set.

where for each measurement the specification limits, the observed mean and standard deviation of the error, the percentage of correct detection (CD) with respect to the specification, the percentage of missed detection (MD) and the false alarm rate (FD) are reported.

It has to be noted that in some cases, the occurrence of a defect may make another measurement impossible. For instance, in Figure 10b, the folded metal blade causes a coarse error in the L_4 measurement. This issue is not important from the standpoint of quality assurance because the piece is definitely to be discarded. The results in Table I do not include the coarse errors.

B. Loose Wire Detection

As previously detailed, the goal of this proposed algorithm is the detection of loose copper wire. In order to evaluate its performance another validation set was collected. It encompassed 40 pieces of which 20 do not present any loose copper wire, while the remaining ones have loose copper wire in different positions. Also in this case the pieces were processed on-line by the system and the operation was repeated 10 times, in order to explore also the repeatability of the system behavior. The performance are summarized in Table II in terms of:

- correct classification percentage (CC) evaluated as the ratio of the pieces correctly classified (with or without loose copper wire) and the number of tests (40x10);
- missed detection percentage (MD) ratio between the number of time in which loose copper wire are not detected and number of tests;
- false detection rate (FD) ratio between the number of time in which good pieces are erroneously recognized with loose copper wire and the number of total tests.

Table I: Summary of the characterization

Type of measurement	**Specification**	**Mean Error E**	**σ_E**	**CD**	**MD**	**FD**
L_1	20.0 ± 1.0 mm	0.01 mm	0.2 mm	100%	0%	0%
L_2, L_2'	1.9 ± 0.5 mm	-0.01 mm	0.3 mm	95%	1%	4%
L_3, L_3'	1.9 ± 0.2 mm	0.02 mm	0.1 mm	100%	0%	0%
L_4, L_4'	2.0 ± 0.5 mm	0.01 mm	0.05 mm	100%	0%	0%
L_5, L_5'	2.0 ± 0.5 mm	0.02 mm	0.7 mm	94%	2%	4%
L_6, L_6'	0.8 ± 0.2 mm	0.01 mm	0.3 mm	99%	0%	1%
α , α’	> 0°	2°	5°	100%	0%	0%
w, w’	< 4.6 mm	0.20 mm	0.9 mm	100%	0%	0%
h, h’	< 1.9 mm	-0.05 mm	0.3 mm	98%	0%	2%
D	< 1.5 mm	0.10 mm	0.4 mm	97%	3%	0%

Table II: Loose wire detection performance

CD	MD	FD
95.0%	4.5%	0.5%

C. Processing time

The processing time of the proposed measurement system is approximately 300 ms, using an ordinary industrial PC (i7, 4 GB RAM). This value allows to monitor 100% of the produced pieces without slowing down the actual production rate.

VI. CONCLUSION

In this paper, an image based inspection system has been described. The system performs dimensional measurements of critical lengths on electromechanical parts. The model for the measurement and the analytical development for error correction have been described. The system currently operates in a production line of the Bitron plant of Alatri, Italy. An important issue authors had to cope with is the requirement of the online operation of the system: it must not introduce significant delays in the timing of the production sequence. The measurement system has demonstrated to be efficient and to fully meet the specifications of the industrial quality production control system. Moreover, this on-line contactless solution has caused a drastic reduction of production waste, and then a decrease of the associated costs.

REFERENCES

[1] Shetty D., Eppes, T, Campana, C , Filburn, T., Nazaryan, N., New approach to the inspection of cooling holes in aero-engines,Optics and Lasers in Engineering, Volume 47, Issue 6, June 2009, Pages 686-694

[2] Liu, Y., Yu, F., Automatic inspection system of surface defects on optical IR-CUT filter based on machine vision, Optics and Lasers in Engineering, Volume 55, 1 April 2014, Pages 243-257.

[3] Rosati, G. Boschetti, G., Biondi, A., Rossi, A., On-line dimensional measurement of small components on the eyeglasses assembly line, Optics and Lasers in Engineering. Volume 47, Issues 3–4, March–April 2009, Pages 320–328

[4] Xie, Y. , Ye, Y., Zhang, J., Liu, L., Liu, L., A physics-based defects model and inspection algorithm for automatic visual inspection, Optics and Lasers in Engineering, Volume 52, Issue 1, 2014, Pages 218-223.

[5] C. Liguori, A. Paolillo, A. Pietrosanto, “An on-line stereo-vision system for dimensional measurement of rubber extrusions”. Measurement 35, 2004, 221-231.

[6] G. Acciani, G. Brunetti, G. Fornarelli, “Application of Neural Networks in Optical Inspection and Classification of Solder Joints in Surface Mount Technology”, IEEE Transactions on Industrial Informatics, Volume:2 , Issue: 3, 2006, 200 – 209.

[7] R. Anchini, G. Di Leo, C. Liguori, A. Paolillo, "Metrological Characterization of a Vision-Based Measurement System for the Online Inspection of Automotive Rubber Profile", IEEE Transactions on Instrumentation and Measurement, Vol. 58 , no. 1, 2009, pp. 4-13..

[8] M. De Santo, C. Liguori, A. Paolillo, A. Pietrosanto: “Standard uncertainty evaluation in image-based measurements”, Measurement, Vol. 36, N: 3-4, October - December, 2004, pp. 347-358.

[9] Hemming, B., Fagerlund, A., Lassila, A., High-accuracy automatic machine vision based calibration of micrometers, Measurement Science and Technology, 2007, 18 (5), 058, pp. 1655-1660.

[10] Yi, S., Haralick, R.M., Shapiro, L.G., Error propagation in machine vision Machine Vision and Applications, Volume 7, Issue 2, June 1994, Pages 93-114

[11] G. Di Leo, C. Liguori, A. Paolillo, A. Pietrosanto, “Online visual inspection of defects in the assembly of electromechanical parts” IEEE International Instrumentation and Measurement Technology Conference (I²MTC); Montevideo; Uruguay; 12-15 May 2014, pp.407-411, ISBN: 978-1-4673-6385-3

[12] R.C. Gonzalez. R.E.Woods. “Digital Image Processing”. 3rd ed., Prentice Hall. 2008. Upper Saddle River, NJ. - ISBN: 9780131687288.

[13] A. Criminisi, I. Reid, A. Zisserman, "Single View Metrology," Proceedings of the Seventh IEEE International Conference on Computer Vision, Vol. 1, 1999, pp. 434-441.